Bowdoin College
Bowdoin Digital Commons

Biology Faculty Publications | Faculty Scholarship and Creative Work

1-1-2000

The guanine nucleotide exchange factor trio mediates axonal development in the Drosophila embryo

Jack Bateman
Harvard Medical School

Huidy Shu
University of California, Los Angeles

David Van Vactor
Harvard Medical School

Follow this and additional works at: https://digitalcommons.bowdoin.edu/biology-faculty-publications

Recommended Citation

Bateman, Jack; Shu, Huidy; and Van Vactor, David, "The guanine nucleotide exchange factor trio mediates axonal development in the Drosophila embryo" (2000). *Biology Faculty Publications*. 29.
https://digitalcommons.bowdoin.edu/biology-faculty-publications/29

This Article is brought to you for free and open access by the Faculty Scholarship and Creative Work at Bowdoin Digital Commons. It has been accepted for inclusion in Biology Faculty Publications by an authorized administrator of Bowdoin Digital Commons. For more information, please contact mdoyle@bowdoin.edu, a.sauer@bowdoin.edu.

Neuron, Vol. 26, 93–106, April, 2000, Copyright ©2000 by Cell Press

The Guanine Nucleotide Exchange Factor Trio Mediates Axonal Development in the *Drosophila* Embryo

Jack Bateman,* Huidy Shu,† and David Van Vactor*‡
*Department of Cell Biology and
Program in Neuroscience
Harvard Medical School
Boston, Massachusetts 02115
†Department of Biological Chemistry
University of California, Los Angeles,
School of Medicine
Los Angeles, California 90095

Summary

Recent analysis of Rho subfamily GTPases in *Drosophila* revealed roles for Rac and Cdc42 during axonogenesis. Here, we describe the identification and characterization of the *Drosophila* counterpart of Trio, a guanine nucleotide exchange factor (GEF) that associates with the receptor phosphatase LAR and regulates GTPase activation in vertebrate cells. Mutants deficient in *trio* activity display defects in both central and peripheral axon pathways reminiscent of phenotypes observed in embryos deficient in small GTPase function. Double mutant analysis shows that *trio* interacts with Rac in a dose-sensitive manner but not with Rho. Moreover, reduction of *trio* activity potentiates the phenotype of mutations in the LAR homolog *Dlar*, suggesting that these proteins collaborate in orchestrating the cytoskeletal events that underlie normal axonogenesis.

Introduction

The development of metazoan organisms is dependent upon the coordination of morphogenic events through cell–cell interaction and the control of cell shape. The formation of accurate axonal connections within the developing nervous system is an excellent example. During development, axons must extend along complex trajectories across long distances and encounter many cell surfaces before they reach their correct destinations (reviewed by Tessier-Lavigne and Goodman, 1996; Van Vactor, 1999). It is well established that axonogenesis requires the translation of extracellular guidance information into directed cell motility through the remodeling of a complex, actin-based cytoskeletal machinery at the leading edge membrane (reviewed by Suter and Forscher, 1998). However, the molecular signaling pathways that integrate axon guidance information and orchestrate cytoskeletal dynamics within the growth cone are largely unknown.

The embryonic nervous system of *Drosophila melanogaster* provides a useful model for understanding axon pathfinding in vivo (reviewed by Tear, 1999). During the later stages of embryonic development, motor axons from each hemisegment leave the *Drosophila* ventral nerve cord (VNC) in two large bundles, the segmental nerve (SN) and the intersegmental nerve (ISN), and extend into the periphery. As they approach their respective target muscles, subsets of axons leave the common motor pathways and enter their target muscle fields. For example, the RP neurons of the ISNb branch defasciculate from the ISN at a specific choice point below the ventral muscle field, then extend into their target domain to make specific synaptic contacts. Experiments using cytochalasin D to directly interfere with actin polymerization have shown that ISNb pathfinding is sensitive to disruption of actin dynamics; at low doses of cytochalasin, many ISNb axons fail to enter the ventral domain and instead "bypass" and extend past their targets. However, at higher doses of cytochalasin, ISNb axons begin to lose their forward progress and "stop short" of their targets (Kaufmann et al., 1998). These observations extend previous cytochalasin experiments in other systems (Letourneau and Marsh, 1984; Bentley and Toroian-Raymond, 1986; Chien et al., 1993), providing evidence that different levels of actin dynamics govern motility and guidance choices in the developing nervous system.

Genetic analyses of motor pathway development have identified numerous loci required for ISNb guidance (e.g., Van Vactor et al., 1993; Desai et al., 1996; Fambrough and Goodman, 1996; Krueger et al., 1996; Kaufmann et al., 1998; Winberg et al., 1998; Yu et al., 1998; Wills et al., 1999a, 1999b). Cloning and molecular characterization have shown that many of these genes encode neuronal cell surface proteins, which are predicted to function as receptors or as cofactors involved in interpreting specific guidance cues. One such group of molecules is the family of receptor-like protein tyrosine phosphatases (RPTPs), including the genes *Dlar*, *DPTP69D*, and *DPTP99A*. Loss-of-function mutations in any one of these genes cause relatively mild defects; with *DPTP69D* and *Dlar*, a partially penetrant ISNb bypass is observed, while mutations in *DPTP99A* cause no discernible phenotype (Desai et al., 1996; Krueger et al., 1996). However, a combined mutant background of all three RPTPs causes many ISNb axons to stop short at the entry to the ventral domain in much the same way as increasing doses of cytochalasin D (Desai et al., 1997; Kaufmann et al., 1998). Such mutant analysis implies a role for RPTPs in translating extracellular guidance cues into directed motility in the growth cone.

Recent studies have begun to identify intracellular molecules as strong candidates for communicating guidance information from the cell surface to the actin cytoskeleton. For example, our analysis shows that the RPTP Dlar functions in an antagonistic partnership with the Abelson protein tyrosine kinase (Abl) (reviewed by Gallo and Letourneau, 1999; Lanier and Gertler, 2000). This phosphorylation-dependent mechanism also appears to involve an Abl substrate protein, Enabled, and an actin-binding protein, Profilin (Wills et al., 1999a, 1999b), which associate with each other and influence actin assembly in different systems (Gertler et al., 1990, 1995, 1996; Pistor et al., 1995; Reinhard et al., 1995;

‡To whom correspondence should be addressed (e-mail: Davie@hms.harvard.edu).

Lanier et al., 1999). Although loss of Enabled function generates an ISNb bypass phenotype similar to loss of Dlar alone (Wills et al., 1999a), loss of Abl or Profilin activity results in ISNb growth cone arrest, suggesting a broad role for these two components in supporting growth cone motility (Wills et al., 1999b). While a biochemical circuit involving Dlar, Abl, and Ena appears to play a prominent role in ISNb guidance, it is likely that a complex pathway of other gene products is also involved.

Rho family small GTPases, including Rho, Rac, and Cdc42, are also strong candidates for transducing axon guidance information to the actin cytoskeleton (reviewed by Hall, 1990; Chant and Stowers, 1995). In nonneuronal cells, these molecular switches control distinct types of actin-based cell motility in response to extracellular cues (Ridley and Hall, 1992; Ridley et al., 1992; Nobes and Hall, 1995). In neurons, Rac has recently been shown to mediate the growth cone collapsing activity of Collapsin-1 (Jin and Strittmatter, 1997), a member of the semaphorin family of guidance factors known to act on the actin cytoskeleton (Fan and Raper, 1995). Although cell surface receptors for semaphorins have been defined (reviewed by Van Vactor and Lorenz, 1999), the mechanism of Rac activation in this system is unknown. However, work in nonneuronal systems indicates that small GTPase activation is initiated by the Dbl homology (DH) family of guanine nucleotide exchange factors (GEFs), which allow Rho family GTPases to release GDP and acquire the GTP necessary for the active state. It is thought that association of GEF proteins with complexes that bind the cytoplasmic domains of cell surface receptors provides the necessary link between extracellular cues and GTPase activation (reviewed by Machesky and Hall, 1996; Fischer et al., 1998).

Although several Rac-like genes exist in *Drosophila* (reviewed by Lu and Settleman, 1999), loss-of-function mutations affecting their activity are currently unknown. Thus, genetic analyses of *Drosophila* Rac function have been carried out using a dominant loss-of-function *Drac1*^{N17} transgene, which is capable of binding upstream activators but is unable to enter the active, GTP-bound state, effectively titrating GEF activity away from endogenous wild-type Rac (Feig and Cooper, 1988; Luo et al., 1994; Kaufmann et al., 1998). Neural-specific expression of this transgene causes an ISNb bypass phenotype similar to that of *Dlar* mutants, implying a role for Rac in ISNb guidance (Kaufmann et al., 1998). However, because of the general nature of Rac inactivation in these experiments, it is unlikely that this phenotype reflects the loss of any particular GEF or *rac*-like gene in a specific signaling pathway. Rather, *Drac1*^{N17} expression likely mimics a partial loss of Rac activation in multiple neuronal guidance events. Thus, in order to understand Rac signaling in the context of specific biochemical pathways, it is necessary to identify and characterize distinct activators of Rac GTPases.

Here, we describe a *Drosophila* homolog of Trio, a multidomain protein containing two DH domains whose vertebrate counterpart specifically activates Rac and Rho (Debant et al., 1996). A close relative of Trio has also been identified in *C. elegans* (*unc-73*; Steven et al., 1998), in which mutant analysis reveals a variety of axon guidance and cell migration phenotypes (Siddiqui and Culotti, 1991; McIntire et al., 1992). Our analysis demonstrates that *Drosophila trio* mediates the development of multiple embryonic axon pathways. Together with data from a companion paper (Liebl et al., 2000 [this issue of *Neuron*]), genetic analysis in *Drosophila* reveals potent genetic interactions between *trio* and a number of signaling components thought to control actin dynamics, including Rac, Dlar, and components in the Abl tyrosine kinase pathway.

Results

The Isolation of *Drosophila trio*

Our strategy to isolate *Drosophila* cDNAs with sequence similarity to human Trio (hTrio) began with the design of degenerate oligonucleotide primers based on conserved sequences between hTrio, a putative *C. elegans* trio homolog (that has since been shown to be UNC-73), and other diffuse b cell lymphoma (Dbl) family exchange factors. Three primers were used in two overlapping polymerase chain reactions (PCRs), with 0–24 hr embryonic cDNA as template, under a variety of reaction conditions (see Experimental Procedures). Reaction products were hybridized on Southern blots at low stringency with radiolabeled hTrio probes, and positive fragments were subcloned and sequenced. The initial clones showed high levels of sequence conservation with hTrio and lower levels with UNC-73, and were therefore used as probes to isolate full-length clones from independent *Drosophila* cDNA libraries. Additionally, BLAST searches of the Berkeley *Drosophila* Genome Project (BDGP) provided several cDNAs from which matching expressed sequence tags (ESTs) had been generated. Completed analysis from three overlapping clones provided roughly 8 kb of contiguous cDNA sequence containing a single open reading frame (ORF) of 6792 nucleotides that predicts a peptide of 2264 amino acids. The predicted initiator methionine for this ORF is preceded by multiple stop codons in the same reading frame. Furthermore, Northern blot analysis at high stringency with full-length cDNA probes identified a single embryonic transcript of $\sim$8 kb (Figure 1B), suggesting that we isolated the entire coding sequence.

To determine whether we had idenified the *Drosophila* counterpart of Trio, we compared the predicted peptide sequence of this ORF to the sequence of hTrio, its close relative, Kalirin (Alam et al., 1997), and UNC-73, as well as other less related proteins. Analysis of the *Drosophila* sequence using BLAST and PFAM algorithms predicts the presence of seven N-terminal spectrin-like domains (residues 313–1227) followed by a DH domain (DH1, residues 1287–1486), a pleckstrin homology domain (PH1, residues 1493–1581), a Src-homology 3 domain (SH3, residues 1645–1708), a second DH domain (DH2, residues 1945–2122), and a second PH domain (PH2, residues 2136–2245) (Figure 1). Both DH domains contain all of the highly conserved residues in the GTPase-binding surface shown to be functionally important by site-directed mutagenesis (Liu et al., 1998) and are thus likely to be enzymatically functional (Figure 1B).

The relative amino acid identity for each domain and

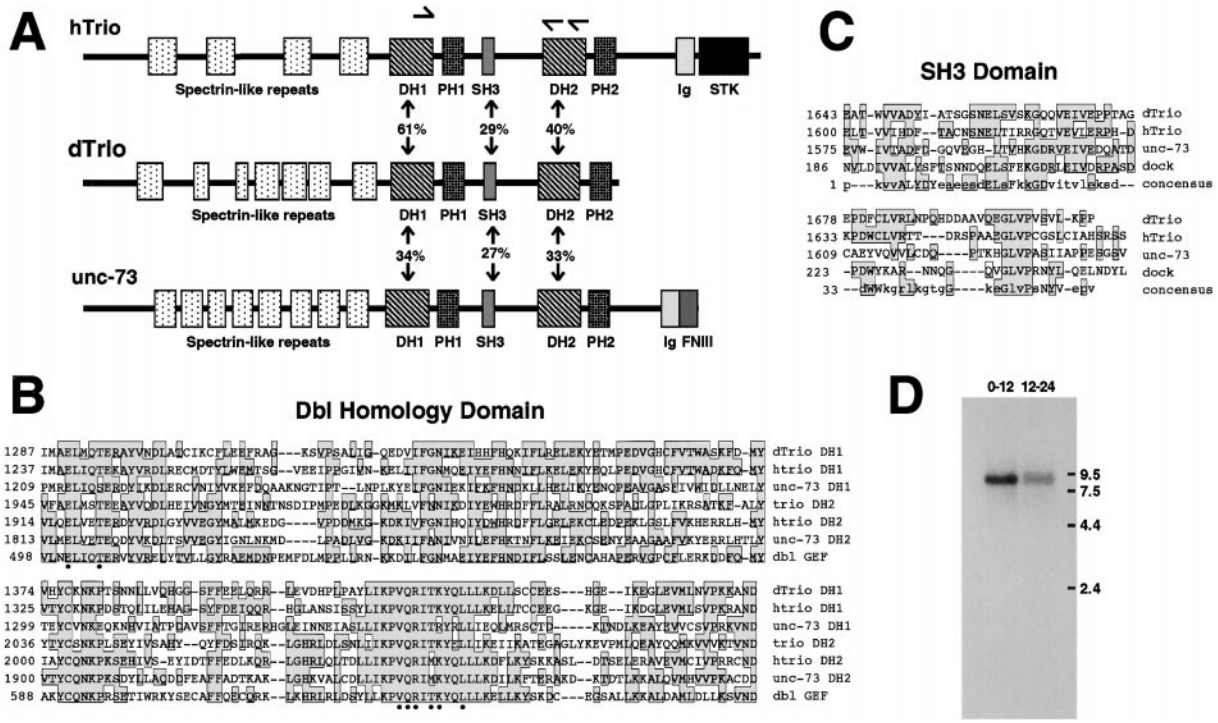

Figure 1. *Drosophila trio* Is a Member of the Trio Family of GEFs

(A) Domain structure of Trio family members from human (hTrio), *Drosophila* (dTrio), and *C. elegans* (UNC-73). All Trio family members share a series of N-terminal spectrin-like repeats followed by tandem DH and PH domains, an SH3 domain, and a second DH/PH pair. Although *trio* coding sequence ends after PH2, hTrio further encodes an Ig domain and a serine/threonine kinase, while UNC-73 enodes an Ig domain and an fibronectin III motif. Half arrows above hTrio indicate the relative positions of degenerate primers used to isolate partial *trio* sequences. Percent identity between DH and SH3 domains of different family members are indicated.

(B) Multiple sequence alignment of Trio DH domains. Sequences of the first and second DH domains from human, *Drosophila*, and *C. elegans* are aligned with the canonical DH domain from the human Dbl oncogene. Identical residues are boxed in shadow. Black dots indicate highly conserved residues shown to be critical for exchange activity by site-directed mutagenesis (Liu et al., 1998).

(C) Multiple sequence alignment of Trio SH3 domains and an SH3 consensus sequence. Included is the SH3 domain from *dreadlocks* (*dock*), an SH2/SH3 adapter protein that shows highest similarity to the SH3 domain of *trio*.

(D) Northern blot analysis of *trio*. Equal amounts of total RNA from 0–12 hr or 12–24 hr embryos were resolved on formaldeyde agarose gels and subjected to Northern blotting. A single transcript of 8–8.5 kb is observed in greater abundance in earlier embryos, consistent with a substantial maternal load. Probes from different regions of the *trio* cDNA yielded identical results.

the organization of these domains reveal that the *Drosophila* sequence is not only conserved in overall structure with members of the Trio GEF family, but is in fact most closely related to hTrio (Figure 1). We therefore refer to this gene as *Drosophila trio*. Despite the close relationship between these family members in fly, human, and worm, all proteins of this family are divergent in their extreme C-terminal domains. Although *Drosophila* Trio contains only 15 residues C-teminal to the PH2 domain, hTrio contains a serine/threonine kinase domain in this position (Debant et al., 1996), whereas UNC-73 lacks the kinase and instead contains a fibronectin-like domain (Steven et al., 1998). The functional significance of this diversity is currently unknown.

trio Is Expressed during Embryonic Development

Since our interest in *trio* function was focused initially on the embryonic nervous system, it was important to explore the expression of the gene during embryogenesis. Northern analysis showed that the *trio* mRNA is present in both 0–12 hr and 12–24 hr embryonic RNA samples (Figure 1D), with the amount of message highest early in development. To examine the distribution of *trio* mRNA in embryonic tissues, we performed whole-mount in situ hybridizations with digoxygenin-labeled antisense RNA probes (as described in Van Vactor and Kopczynski, 1999). Probes from both the 5′ untranslated region and the DH1 domain yielded identical patterns of expression.

Consistent with the Northern analysis, *trio* is abundant and ubiquitous early in embryogenesis (stages 4–6; Figure 2A); this indicates a substantial maternal contribution. At stages 11–12, *trio* message is broadly distributed, with highest levels in invaginating gut (anterior and posterior) and in a repeating pattern within the developing central nervous system (CNS) (Figure 2B). At stages 13–15, CNS expression is maintained at high levels, while a new pattern of epidermal expression at segment boundaries emerges (Figures 2C, 2E, and 2F). This peripheral staining corresponds to the epidermal muscle attachment (EMA) cells, a specialization of the body wall epidermis involved in patterning and maintaining

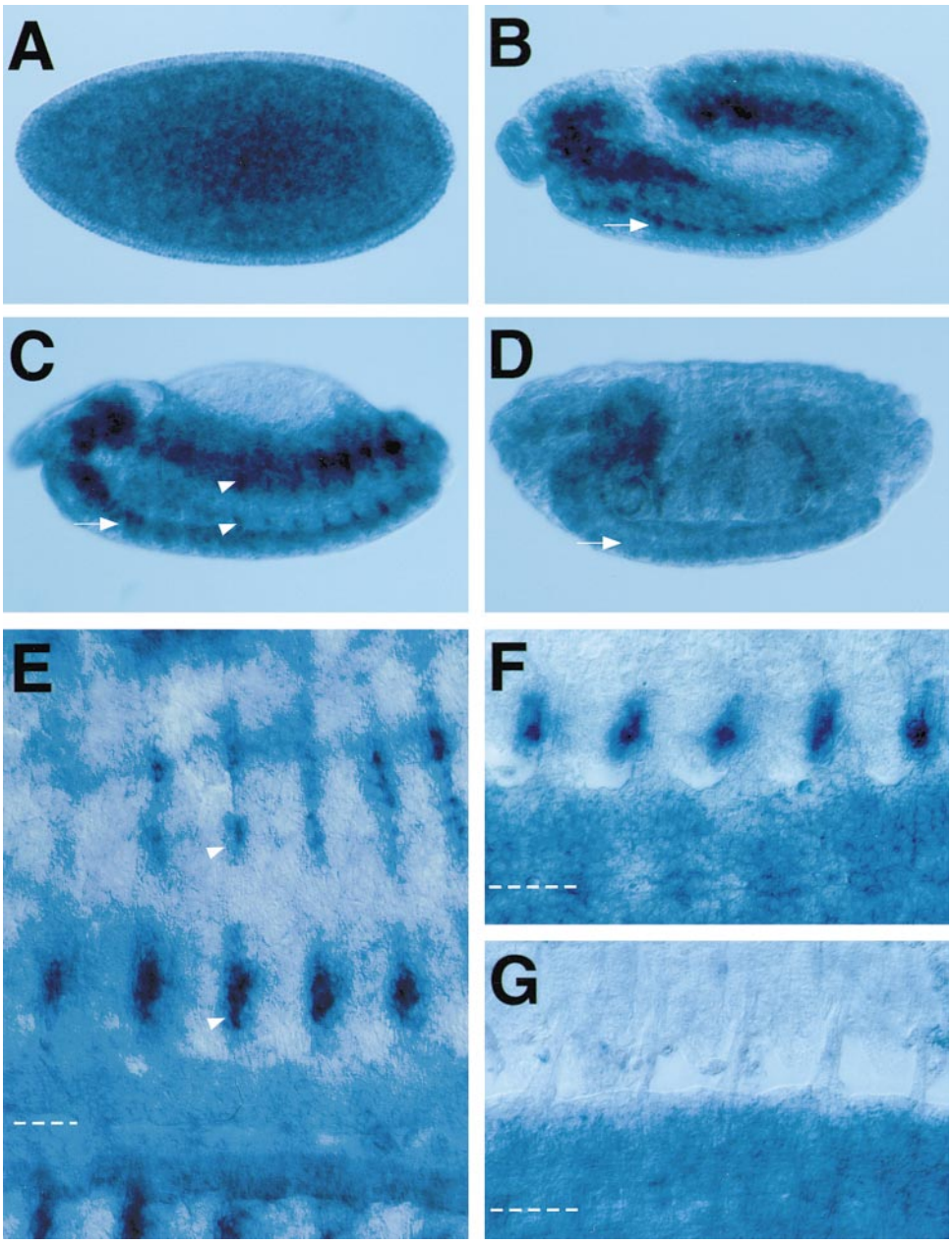

Figure 2. Expression of *trio* during Embryonic Development

Embryos were prepared for in situ hybridization as described (Van Vactor and Kopczynski, 1999) using digoxyenin-labeled RNA probes from either DH1 or the 5′ UTR. Controls performed in parallel using a heterologous probe showed no overlap in staining pattern (data not shown). In all panels, anterior is to the left, and dorsal is toward the top of the page.

(A) An early (stage 5) embryo showing significant staining, indicative of a substantial maternal contribution. Preblastoderm embryos show similar or stronger staining.

(B) In more mature embryos (stage 11), a background of general staining is still present; however, a significantly stronger signal is observed in the developing CNS (arrow) and gut.

(C, E, and F) At stage 13, expression in the CNS (arrow) and gut continues, while a new pattern of expression is observed at segment borders of the epidermis (EMA cells, arrowheads in [C] and [E]). (E) and (F) show increasing magnifications of a filleted stage 13 embryo showing strong CNS and EMA cell staining. The dotted line indicates the ventral midline of the embryo.

(D and G) At stage 16, EMA cell and gut expression are reduced to background, while slightly higher expression is maintained in the CNS (arrow). (G) shows a filleted stage 16 embryo, as described above.

Scale bar, approximately 100 μm (A–D); 40 μm (E); and 30 μm (F and G).

the integrity of muscle attachment sites (Bate, 1993). EMA cell expression is transient and is undetectable by stage 16, while CNS expression is maintained at a reduced level throughout stage 16 (Figures 2D and 2G). The abundant and sustained expression of *trio* RNA in the developing CNS is consistent with a role in axonogenesis.

Genetic Screens Identify Mutations in the *trio* Gene

To initiate a genetic analysis, we mapped the *trio* transcription unit to the 61E region of chromosome 3 by hybridization to an existing array of *Drosophila* genomic P1 clones (see Experimental Procedures). This location was confirmed by sequence comparison with several mapped sequence tagged sites from the BDGP that overlap with the *trio* cDNA. Several *Drosophila* strains carrying P element insertions in the 61D-F region had been previously isolated (Deak et al., 1997). Using inverse PCR on genomic templates from these strains, we isolated DNA fragments that flank each P element insertion site. Hybridization of inverse PCR products and fragments from the *trio* cDNA to Southern blots of genomic P1 clones digested with several restriction enzymes identified two independent P element insertions in close proximity to the 5′ end of *trio*. We further mapped each insertion relative to the putative transcriptional start site using PCR and sequence analysis (see Experimental Procedures). The insertions *P[1372/3]* and *P[1386/6]* lie within 5 bp of one another in the predicted first exon of the *trio* transcript (Figure 3B), corresponding to the 5′ untranslated region. The position of the P elements raised the possibility that these insertions interfere with *trio* expression.

Consistent with the disruption of a common gene, both P element insertions are semilethal and generate adult "escapers" with an identical wing posture phenotype. In genetic crosses in which we followed the wing phenotype, both insertion alleles fail to complement each other and the deficiency *Df(3L)Ar12-1*, which spans 61E. Moreover, excision of the *P[1372/3]* insertion (see Experimental Procedures) generated revertants whose viability and wing posture were restored to normal, demonstrating that the phenotypes were insertion dependent. To determine whether the adult phenotypes were due to loss of *trio* function, we first examined *trio* expression on Northern blots of adult mRNA. While *trio* message was detected easily in heterozygous (*P[1372/3]/+*) adults, no signal was detected in homozygous escapers (*P[1372/3]/P[1372/3]*) (Figure 3C). Densitometric scans of multiple blots showed that *trio* mRNA levels are reduced at least 10-fold in the mutant relative to wild-type. Furthermore, in situ hybridization of mutant embryos derived from homozygous mutant mothers (*P[1372/3]/P[1372/3]*) showed a strong reduction in staining both for maternal contribution and neural expression, consistent with a >10-fold reduction in message.

To obtain more conclusive evidence that the mutant defects resulted from loss of *trio* activity, we constructed a transgenic strain in which a full-length wild-type *trio* cDNA could be expressed under the control of the GAL4 upstream activating sequence (UAS), as described by Brand and Perrimon (1993). Expression of this transgene with the epidermal GAL4 driver T155 substantially rescued the wing posture phenotype of mutant adults. For example, *T155-GAL4,P[1386/6]/Df(3L)Ar12-1* adults show 91% wing phenotype (n = 98); however, *UAS-trio/+;T155-GAL4,P[1386/6]/Df(3L)Ar12-1* adults show only 17% wing phenotype (n = 92). Thus, we have identified the *trio* complementation group and will refer to the P element lines as $trio^{1372/3}$ and $trio^{1386/6}$.

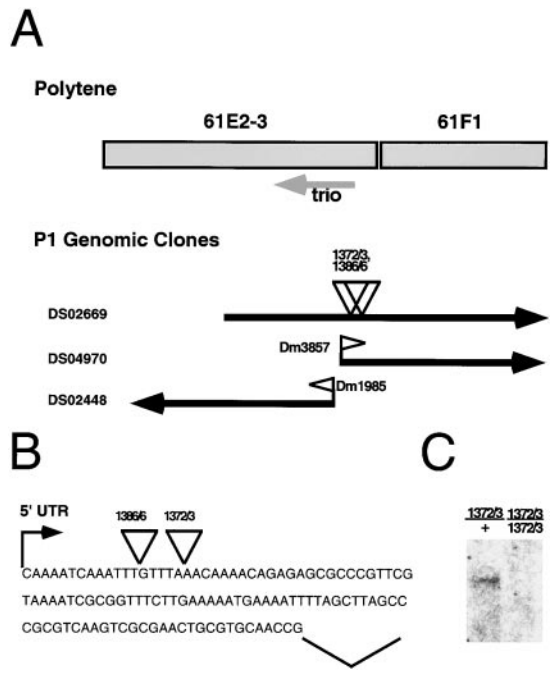

Figure 3. P Element Insertions that Disrupt *trio*

(A) The position of the *trio* transcript (shaded arrow) is given relative to the polytene chromosome in region 61E. Of several overlapping P1 genomic clones that span the region (closed arrows), two have been used to generate STSs (open flags) that correspond to Trio coding sequence. The relative position of P element insertions *P[1372/3]* and *P[1386/6]* (triangles) is given based on hybridization to digested P1 DNA.

(B) P element insertion sites were further mapped to the putative first exon of the *trio* transcript by PCR and sequence analysis. The predicted transcriptional start site is shown with an arrow, and the first splice junction is indicated.

(C) The P element *P[1372/3]* disrupts the *trio* locus. Equivalent amounts of RNA from heterozygous (left lane) or homozygous (right lane) adults bearing the P element insertion were probed with a radiolabeled, full-length Trio cDNA. While the 8 kb transcript is observed in heterozygotes, no transcript is detected in homozygous flies. Densitometric scans of three independent blots showed background levels of 8.5%, 9.8%, and 16.5% of wild-type signal, which sets an upper limit for mutant mRNA levels by this analysis.

In a parallel set of experiments, we undertook a saturation mutagenesis of the region 61D3-61F8, covered by $Df(3L)bab^{PG}$, using the mutagen ethyl methanesulfonate (EMS), which generates primarily point mutations. From a screen of 7410 lines, 97 independent lethal mutations were recovered (see Experimental Procedures); 27 of these alleles fail to complement the smaller deficiency, *Df(3L)Ar12-1*, and were thus candidate *trio* alleles. Complementation crosses of each lethal EMS mutation to $trio^{1386/6}$ revealed 10 novel alleles that failed to complement *trio* for either viability or wing posture and are thus considered mutations in the *trio* complementation group.

To gain further evidence that the EMS mutations disrupt *trio* function, we attempted to rescue the lethality of strong mutant alleles by simultaneously expressing a *UAS-trio* transgene in postmitotic neurons using the GAL4 driver *elaV-GAL4*. For example, while $trio^{6A}$/*Df(3L)Ar12-1* embryos very rarely survive to pupal stages

Table 1. Quantitation of Axonal Defects in *trio* Mutant Embryos

Genotype	Axon Pathway Phenotype ISNb Stop Short[a]	SNa Stop Short[b]	CNS Fascicle Break	
w^{1118}	2.0% (n = 118)	0.0% (n = 322)	1.2% (n = 320)	wild-type
$trio^{BX4}/trio^{1386/6}$	2.8% (n = 71)	0.0% (n = 102)	1.2% (n = 160)	control
$trio^{6A}/trio^{15B}$	10.6% (n = 123)	6.2% (n = 96)	30.5% (n = 210)	LOF
$trio^{6A}$/*Df(3L) Ar12-1*	16.8% (n = 178)	1.9% (n = 210)	20.8% (n = 322)	LOF
$trio^{2H}$/*Df(3L) Ar12-1*	18.5% (n = 157)	6.3% (n = 189)	31.3% (n = 392)	LOF
$trio^{1372/3}/trio^{1372/3}$	23.0% (n = 135)	7.3% (n = 150)	20.6% (n = 266)	LOF
$trio^{1372/3}/trio^{1386/6}$	23.1% (n = 95)	3.2% (n = 186)	15.4% (n = 240)	LOF
$trio^{1372/3}/trio^{BX1B}$	22.1% (n = 181)	5.9% (n = 135)	14.6% (n = 308)	LOF
P[UAS-trio]6B;$trio^{1372/3}/trio^{BX1B}$*, P[elaV-GAL4]*	6.2% (n = 64)	0.0% (n = 52)	2.0% (n = 98)	LOF + cDNA

Note: n = number of embryonic hemisegments (abdominal A2-A7); Alleles: *1372/3* and *1386/6* are P element insertions in the gene; *BX1B* is an imprecise excision; *2H, 6A* and *15B* are lethal point mutant alleles; *Df(3L)Ar12-1* completely removes the gene; and *BX4* is a precise excision that restores the *trio* locus to normal.

[a] ISNb branches were scored as abnormal when the distal muscle 12 was not innervated (mutant ISNbs often stopped even earlier);

[b] SNa branches were scored as abnormal if either the dorsal or lateral trajectory terminated prior to target contact. Abbreviation: LOF, loss-of-function.

(1.5%, n = 173 of expected nontubby pupae from the cross $trio^{6A}$*/TM6B,Tb* × *Df(3L)Ar12-1/TM6B,Tb)*, neural expression of *trio* fully rescues the early larval lethality of this mutant combination (100%, n = 147 of expected). These pupae develop to late stages but fail to eclose as viable adults, suggesting some *trio* function outside of the nervous system. However, since neural expression extends the lethal phase of strong allelic combinations, the early lethality of *trio* mutants is due to a loss of activity in the nervous system.

Analysis of *trio* Mutants Reveals Defects in Multiple Axon Pathways

Having defined a collection of independent alleles, we were in a position to examine the *trio* loss-of-function phenotype during embryonic nervous system development. To assess the development of different axon pathways, embryos from different allelic combinations were collected and stained with the anti-Fasciclin II (Fas II) antibody mAb 1D4, an excellent marker for motor axon pathways (Van Vactor et al., 1993), and specific fascicles of longitudinal axons (Lin et al., 1994).

Analysis of motor axon pathfinding revealed defects in the ability of nerve branches to reach their target muscles in *trio* mutants. The two branches most sensitive to perturbation of small GTPase function, ISNb and SNa (Kaufmann et al., 1998), were also most sensitive to the loss of *trio* activity. These phenotypes were observed in all allelic combinations tested, with some variation in penetrance depending on genetic background (Table 1). Occasionally, we observed defects in target muscle attachment to the underlying epidermis, which likely reflects a role for *trio* in EMS cells. To avoid scoring guidance errors that could be caused by the target rather than the growth cone, we excluded all segments with abnormal muscle patterning from our analysis.

Most predominantly, we observed a failure of ISNb growth cones to reach their distalmost target, muscle 12 (Figure 4; Table 1). For example, in $trio^{1372/3}/trio^{1372/3}$ embryos, 23% (n = 135) of stage 17 A2–A7 hemisegments show an ISNb "stop short" phenotype, while wild-type embryos seldom display this defect (2%, n = 118). Many projections that successfully contacted muscle 12 in *trio* mutants were themselves abnormally thin and diminutive but were not included in our quantitative analysis (see Experimental Procedures). Occasionally, ISNb axons were seen stalled at the entry to the ventral domain, as has been observed with strong doses of cytochalasin D (see Introduction), consistent with a loss of growth cone motility. However, it is unlikely that all observed defects reflect a general growth cone arrest, as some ISNb projections were observed extending beyond their normal innervation site on muscle 12, making inappropriate contacts on nontarget muscles (data not shown). Similarly, ISNb axons were sometimes observed extending anteriorly or posteriorly between muscles 14 and 28 rather than entering the ventral domain. Thus, while some mutant ISNb growth cones may lose their ability to maintain forward progress, others seem to be defective in responding normally to guidance information.

To ensure that the observed defects in ISNb guidance resulted from the loss of *trio*, we examined embryos carrying $trio^{BX4}$, a precise excision of the *P[1372/3]* insertion that restores the locus. These embryos displayed wild-type levels of ISNb stop short (2.8%, n = 71 for $trio^{BX4}/trio^{1386/6}$), demonstrating that the phenotype was insertion dependent.

The defects observed in SNa development were similar to those of the ISNb phenotype. In *trio* mutants, SNa sometimes fails to extend either its lateral branch, to contact muscles 5 and 8, or its vertical branch, to contact longitudinal muscles 21–24 (Figure 4). Occasionally, SNa fails to reach its target domain altogether, instead stalling beneath the ventral target domain of ISNb. Although not highly penetrant, these SNa defects were seen in all allelic combinations examined but not in wild-type or precise excision controls (Table 1).

Consistent with defects observed in motoneurons, analysis of axon trajectories in the CNS revealed an inability of axons to pathfind correctly. During early development of the CNS, longitudinal axons are required to cross segment boundaries and extend into neighboring segments, such that by the late stages of embryonic development (stage 17), distinct 1D4-positive fascicles form continuous pathways along the length of the CNS (Figure 5A). In mutant embryos lacking *trio* function, we observed defects in the formation of these pathways.

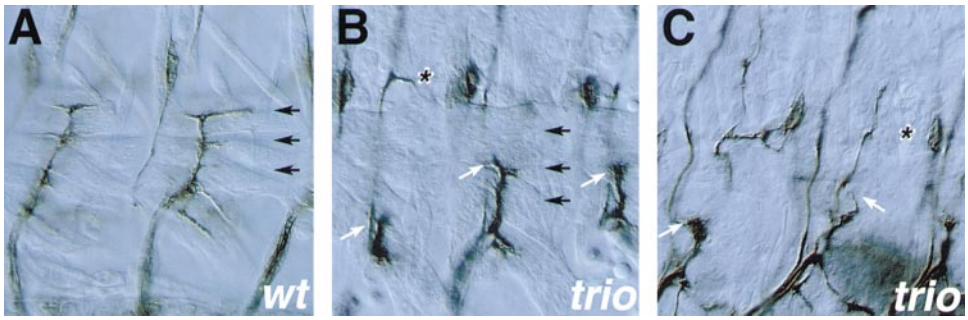

Figure 4. *trio* Is Required for Motor Axon Pathfinding

(A) The wild-type pattern of ISNb innervation is shown in two hemisegments of a stage 17 filleted embryo stained with mAb 1D4. Closed arrows indicate stereotyped innervations of the ventral muscles, with the distalmost innervation of target muscle 12 being highest on the page.

(B) In *trio* mutants, ISNb axons frequently fail to reach their targets. Three hemisegments of a late stage 16 fillet are shown (genotype, $trio^{1372/3}$/$trio^{1386/6}$), when all ventral muscles should be contacted. Open arrows indicate arrested ISNb projections. The segment to the left represents an early stop short phenotype at the choice point, while the two segments to the right show projections that have entered the ventral domain but fail to extend to muscle 12. Additionally, the SNa projection of the leftmost segment has arrested at a lower plane of focus (see [C]), while an ectopic collateral projection from the ISN invades the SNa target region (asterisk).

(C) Mutations in *trio* affect SNa projections. The wild-type pattern of SNa innervation is shown in the left segment of this stage 17 fillet (genotype, $trio^{1372/3}$/*Df(3L)Ar12-1*) at a slightly deeper plane of focus than in (A) and (B). In the segment to the right, the branch projecting back to target muscle 8 is not visible (asterisk). Aberrant ISNb projections are also visible in this plane of focus (open arrows), although their target muscles are not.

The most dramatic and persistent disruption was seen in the lateralmost Fas II–positive longitudinal pathway, where we often observed breaks and/or inappropriate direction of these interneuronal axons (Figure 5). In $trio^{1372/3}$/$trio^{1372/3}$ embryos, 20.6% of stage 17 A2–A8 hemisegments (n = 266) failed to connect to the neighboring segment, compared with only 1.2% (n = 320) in wild-type embryos. Similar defects were seen in multiple allelic combinations (Table 1). Similar embryonic phenotypes are described in a companion paper (Awasaki et al., 2000 [this issue of *Neuron*]), providing independent confirmation of our results.

trio Is Required in Postmitotic Neurons for Axon Pathway Formation

We have shown that mutations in *trio* cause specific defects in the formation of multiple embryonic axon pathways, implying a role for *trio* activity in developing axons. However, because *trio* expression is not restricted to neurons, it is possible that its activity is required elsewhere and that the axonal phenotypes observed represent functions outside the nervous system. To exclude this possibility, we analyzed axon pathway formation in mutant embryos while simultaneously expressing a wild-type *trio* construct in postmitotic neurons using the GAL4 driver *elaV-GAL4*. These embryos show a marked reduction in pathfinding errors in both the CNS and the motor nervous system (Table 1), indicating that the axonal defects in *trio* mutants result from a lack of *trio* function in neurons.

trio Displays Dose-Sensitive Interactions with Rac

Cell transfection and in vitro nucleotide exchange assays with each DH domain of hTrio suggested that GEF1 preferentially activates Rac, whereas GEF2 activates Rho (Debant et al., 1996; Bellanger et al., 1998a). To explore the relationship between *trio* and Rac in *Drosophila*, we used the compound eye as an established system to test for genetic interactions in GTPase signaling pathways (Barrett et al., 1997; Nolan et al., 1998). Rac overexpression under the control of the eye-specific promoter GMR creates a mispatterened "rough" eye in which individual ommatidia are misshapen (Figure 6B). However, removal of a single copy of *trio* caused a dramatic suppression of this Rac gain-of-function phenotype (Figures 6C and 6D). This was true for additional *trio* alleles (data not shown). In contrast, overexpression of Rho also generates a rough eye (Figure 6E), but this phenotype was not significantly altered by reduction in *trio* activity (Figure 6F). This suggested that in the *Drosophila* retina, *trio* functions to activate one or more of the *Drosophila* Rac-like genes but not Rho.

In the embryo, previous studies showed that the same nerve branches affected by *trio* mutations were also most sensitive to Rac perturbation (Kaufmann et al., 1998). Although occasional ISNb stop short phenotypes are observed, the predominant ISNb and SNa bypass phenotypes induced by $Drac1^{N17}$ overexpression are distinct from phenotypes caused by loss of *trio* function. This difference likely reflects $Drac1^{N17}$ interference with multiple neural activators of Rac GTPases. However, we reasoned that if *trio* is involved in Rac activation in the embryonic motor nervous system, the penetrance of the $Drac1^{N17}$ phenotype should be sensitive to changes in the genetic dose of *trio*. Consistent with this hypothesis, removal of a single copy of *trio* in embryos expressing $Drac1^{N17}$ caused a distinct increase in the penetrance of ISNb bypass (Table 2). This was true for all alleles of *trio* tested. Moreover, coexpression of $Drac1^{N17}$ and a wild-type *trio* transgene resulted in a dramatic suppression of the ISNb bypass phenotype, consistent with the model that *trio* is an activator of Rac GTPases in the embryonic motor nervous system. Because expression of the analogous $DRho1^{N19}$ does not cause specific neural guidance errors, we were unable to address whether

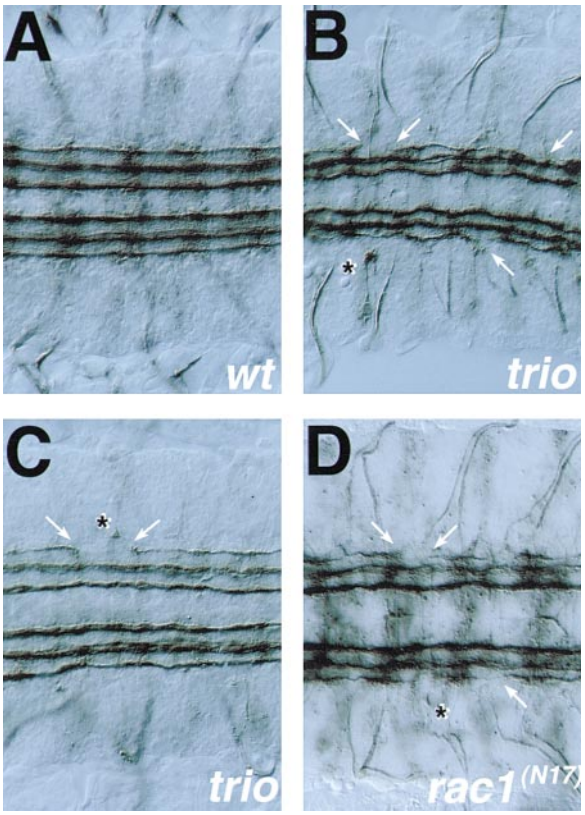

Figure 5. *trio* Mutants Display CNS Defects Similar to those of Rac Dominant-Negative

All panels show stage 17 fillets stained with mAb 1D4, with the anterior–posterior axis running from left to right.

(A) A wild-type embryo showing distinct unbroken longitudinal fascicles.

(B and C) In *trio* mutants, longitudinal axons of the lateralmost fascicle frequently fail to cross segment boundaries (open arrows) and are often observed turning toward the periphery or collapsing on more medial pathways before arresting. Additionally, misrouted ID4-positive axons are often observed outside the longitudinal pathways (asterisks). The genotypes of the embryos shown are $trio^{1372/3}/trio^{1386/6}$ in (B) and $trio^{1372/3}/Df(3L)Ar12\text{-}1$ in (C).

(D) An identical phenotype is observed in embryos expressing the dominant-negative $Drac1^{N17}$ with the postmitotic neural driver C155-GAL4, including failed connections of the lateralmost pathway (arrows) and ectopic 1D4 staining (asterisk).

dosage-sensitive interactions exist in Rho family signaling. However, removal of one copy of *trio* in embryos expressing $Dcdc42^{N17}$ did not alter the penetrance of ISNb stop short in this background (data not shown). Thus, the genetic interactions observed between *trio* and $Drac1^{N17}$ are specific to the Rac family of GTPases.

Despite phenotypic differences between $Drac1^{N17}$ and *trio* in the motor nervous system, analysis of the CNS in embryos lacking Rac function reveals defects identical to those observed in *trio* mutants. Specifically, expression of the dominant-negative $Drac1^{N17}$, under the control of the neural-specific GAL4 driver C155, caused a failure of the lateralmost Fas II–positive longitudinal pathway to properly connect at stage 17 (13.7%, n = 168) (Figure 5D). In contrast, neural expression of either $Dcdc42^{N17}$ or $DRho1^{N19}$ does not cause defects in longitudinal pathfinding, indicating that the CNS phenotype is specific to interference with Rac-like GTPase function. Thus, in the CNS, mutant phenotypes of $Drac1^{N17}$ and *trio* are consistent with disruption of a common pathway.

Genetic Interactions Suggest that *trio* Collaborates with Dlar

The ISNb and longitudinal pathway defects observed in *trio* mutants are similar to those of phenotypes observed in embryos mutant for the *Abl* tyrosine kinase. In addition, results from a companion paper imply that *Abl* and *trio* function together to control axon guidance at the midline (Liebl et al., 2000). Previous analysis has shown that a partial reduction in *Abl* function suppresses the bypass phenotype caused by mutations in the RPTP *Dlar*, implying an antagonistic relationship between kinase and phosphatase. To address *trio* function at this ISNb choice point, we examined ISNb pathfinding for dosage-sensitive interactions between *Dlar* and *trio*.

In strong zygotic *Dlar* mutants ($Dlar^{13.2}/Dlar^{13.2}$), we observed ISNb bypass at a moderate frequency (18.4%, n = 223 A2–A7 hemisegments). However, partial reduction of *trio* activity in this *Dlar* background ($Dlar^{5.5}/Dlar^{5.5};trio^{1372/3}/+$) enhanced the ISNb bypass ~2-fold (37%, n = 211). The same effect was observed in multiple double mutant allelic combinations (Table 2). Although this potentiation disagrees with a simple model in which *trio* and *Abl* function together to oppose phosphatase signaling, it is consistent with the previous observation that neural expression of $Drac1^{N17}$ enhances the frequency of bypass in *Dlar* mutants (Kaufmann et al., 1998). Thus, although *trio* may collaborate with *Abl* at the CNS midline, it rather appears to cooperate with *Dlar* and *Drac1* during ISNb ventral target entry. The absence of bypass phenotypes in *trio* single mutants is likely to reflect the existence of additional inputs to Rac family GTPases that would be susceptible to the $Drac1^{N17}$ dominant-negative effect.

Discussion

The diversity of morphogenetic events involved in *Drosophila* development, combined with a powerful set of genetic tools, makes this a convenient organism for analysis of the signaling machinery regulating cytoskeletal architecture. Although *Drosophila* Rho family GTPases have been shown to mediate a broad spectrum of developmental events, from axonogenesis (Luo et al., 1994; Sone et al., 1997; Kaufmann et al., 1998) and cell migration (Murphy and Montell, 1996) to epithelial morphogenesis (Harden et al., 1995), cell polarity (Eaton et al., 1995, 1996), and myoblast fusion (Luo et al., 1994), pathways that regulate GTPase activation have been elucidated for very few of these functions (reviewed by Lu and Settleman, 1999). Here, we describe a *Drosophila* homolog of the GEFs Trio and UNC-73. Our analysis of embryonic neuroanatomy reveals a requirement for *Drosophila trio* during the formation of multiple axon pathways. Although other activators of Rho family GTPases have been identified in the *Drosophila* nervous system (e.g., *Son of sevenless*, Simon et al., 1991; *still life*, Sone et al., 1997), *trio* is the first member of this group demonstrated to be required for the initial formation of axon pathways. The multidomain nature of this

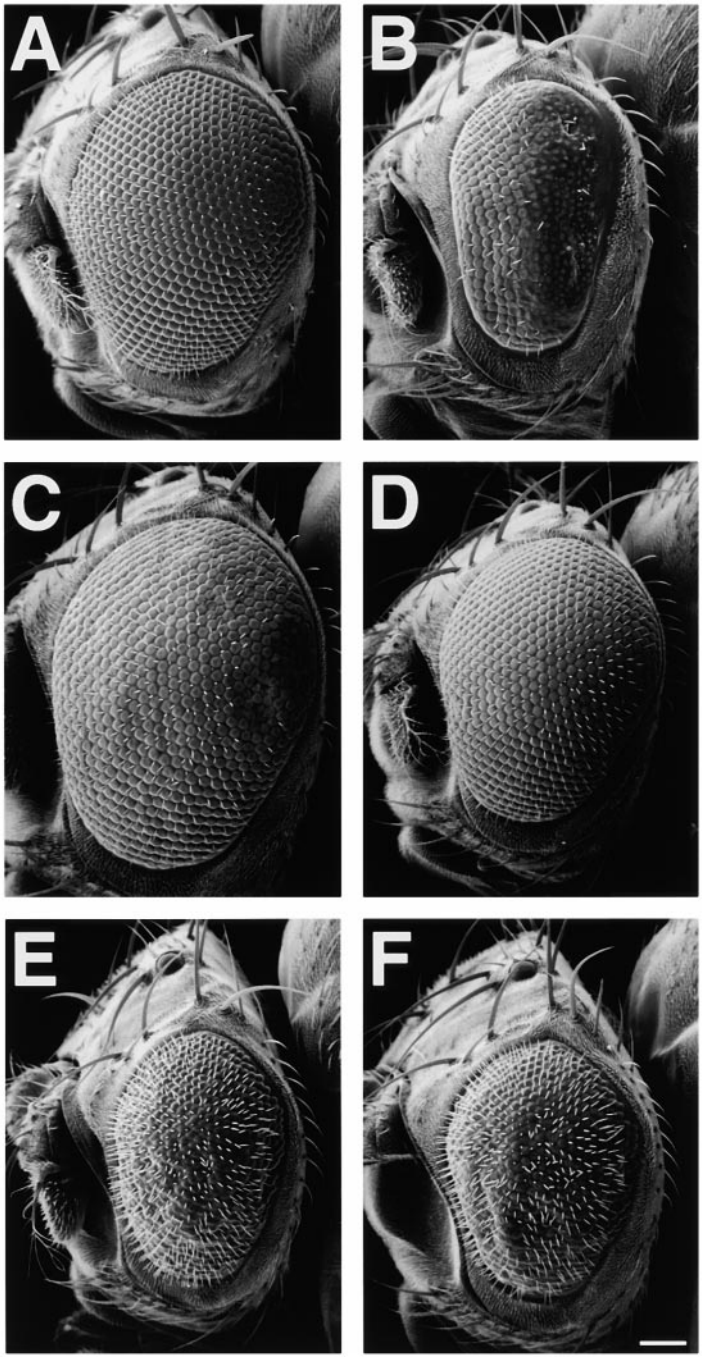

Figure 6. *trio* Interacts with Rac but Not Rho in the *Drosophila* Retina

All panels show scanning electron micrographs of adult *Drosophila* eyes at 200× magnification and are representative of at least ten flies analyzed for each genotype. Scale bar, ~100 μm.

(A) A wild-type compound eye showing organized rows of distinct ommatidia.

(B) The wild-type pattern is severely disrupted by overexpression of Drac1 under the control of the retinal-specific promoter GMR. Many ommatidia are fused or flattened, and the overall shape of the eye is reduced.

(C and D) The disruption caused by Drac1 overexpression is dramatically suppressed by removing a single copy of *trio*. The genotypes presented are *GMR-Drac1/trio*^{2H}, an EMS allele in *trio* (C), and *GMR-Drac1/Df(3L)Ar12-1*, a deficiency for the *trio* locus (D). The same effect has been seen with multiple alleles.

(E) Expression of *DRho1* under the control of the GMR promoter also severely disrupts ommatidial patterning. However, removal of a single copy of *trio* in this background does not appear to affect the disruption (*GMR-DRho1/trio*^{2H}, [F]).

protein makes it well suited to the job of linking different signaling pathways controlling actin cytoarchitecture. Accordingly, *trio* displays genetic interactions with a number of signaling molecules known to collaborate during the guidance of embryonic axons.

Trio and Embryonic Motor Axon Guidance

Our genetic analysis demonstrates a requirement for *trio* function in the formation of pathways both in the CNS and in the motor nervous system. Many of the phenotypes observed are consistent with a general lack of motility, similar to those observed in embryos lacking the actin-binding protein Profilin (Wills et al., 1999b). However, ISNb axons lacking *trio* are frequently capable of extending toward their target, muscle 12, but instead make inappropriate contact with nontarget muscles, indicating an intact forward motility but abnormal guidance. These observations are similar to those of a companion paper examining *trio* function in the visual system, where loss of *trio* activity causes some photoreceptor axons to arrest before reaching their targets, while others project beyond them (Newsome et al., 2000 [the April 28 issue of *Cell*]). Similarly, the phenotypes observed in *unc-73* mutants of *C. elegans* reflect defects

Table 2. Reduction in *trio* Potentiates the *Drac1*^{N17} and *Dlar* Phenotypes

Genotype	Axon Pathway Phenotype ISNb Bypass	
+,*P[elaV-GAL4]*/+,*P[UAS-Drac1*$^{N17.1}$*]*	56.7% (n = 184)	Drac1 DLOF
trio^{Bx1B},*P[elaV-GAL4]*/+,*P[UAS-Drac1*$^{N17.1}$*]*	78.0% (n = 155)	Drac1 DLOF + reduced Trio
trio^{6A},*P[elaV-GAL4]*/+,*P[UAS-Drac1*$^{N17.1}$*]*	87.7% (n = 154)	Drac1 DLOF + reduced Trio
P[UAS-trio^{+}*];P[elaV-GAL4]/P[UAS-Drac1*$^{N17.1}$*]*	12.2% (n = 164)	Drac1 DLOF + elevated Trio
Dlar$^{13.2}$/*Dlar*$^{13.2}$;+/+	18.4% (n = 223)	Dlar LOF
Dlar$^{13.2}$/*Dlar*$^{13.2}$;*trio*$^{1372/3}$/+	37.0% (n = 211)	Dlar LOF + reduced Trio
Dlar$^{5.5}$/*Dlar*$^{5.5}$;+/+	19.5% (n = 159)	Dlar LOF
Dlar$^{5.5}$/*Dlar*$^{5.5}$;*trio*$^{1386/6}$/+	30.5% (n = 128)	Dlar LOF + reduced Trio
Dlar$^{5.5}$/*Dlar*$^{13.2}$;+/+	16.0% (n = 156)	Dlar LOF
Dlar$^{5.5}$/*Dlar*$^{13.2}$;*trio*$^{1372/3}$/+	41.0% (n = 166)	Dlar LOF + reduced Trio

Note: the *Dlar* alleles used in this study are products of extensive recombination to remove all modifier loci and are thus less penetrant than the alleles originally described by Krueger and colleagues (1996). Abbreviations: DLOF, dominant loss-of-function; GOF, gain-of-function; LOF, loss-of-function.

in both axon extension and specific guidance choices (McIntire et al., 1992). These observations are consistent with a model in which Trio functions in one or more signal transduction pathways responsible for conveying guidance information to the growth cone. However, previous experiments using cytochalasin D have shown that distinct levels of actin dynamics are required either for guidance or motility (Kaufmann et al., 1998), raising the question of whether *trio* mutant phenotypes reflect an inability to interpret specific guidance cues or a generally defective cytoskeletal machinery. A more detailed cell biological approach to the study of Trio and other signaling partners will be required to distinguish between these different models.

Previous analyses of embryonic axon guidance in *Drosophila* have shown that multiple signaling pathways converge to ensure the accurate navigation of motor growth cones to appropriate targets (see Introduction). In the case of ISNb guidance, multiple neuronal RPTPs function to bring this small subset of axons to ventral muscles (Desai et al., 1996, 1997; Krueger et al., 1996). Our recent work suggests that at least one of these receptors, Dlar, works in partnership with Rac and components of the Abl tyrosine kinase pathway to control the assembly of the growth cone cytoskeleton (Kaufmann et al., 1998; Wills et al., 1999a, 1999b). In the case of Rac, potent genetic interactions with Dlar suggested that a GTPase activator also regulates ISNb target entry (Kaufmann et al., 1998). Our present genetic analysis allowed us to address *trio* function at the choice point by dosage-sensitive interactions. Although the CNS and ISNb phenotypes caused by lack of *trio* activity are similar to *Abl* and *chic* mutant embryos, *Abl* and *trio* do not appear to cooperate at the ISNb choice point. Rather, while *Abl* kinase activity opposes the action of *Dlar*, loss of *trio* or Rac function potentiates the bypass phenotype of *Dlar* mutants, implying a common role for the phosphatase and the Rac pathway during target entry. A similarly complex relationship is observed between Dlar and DPTP99A; double mutant analysis has shown a cooperative association with regard to ISN and ISNb motility, but opposing function between the phosphatases in ISNb target entry (Desai et al., 1997). These data imply an elaborate interaction of gene functions during axonogenesis that is dependent upon particular guidance choices and cellular contexts.

Consistent with a hypothesis in which *trio* and *Dlar* function in a common pathway, yeast interaction trap assays with the cytoplasmic domain of human LAR identified hTrio as a strong interactor, providing a possible biochemical means of regulating Trio function (Debant et al., 1996). Although hTrio interacts quite well with the cytoplasmic domain of Dlar in the yeast interaction trap assay, *Drosophila* Trio appears to lack the C-terminal domain that mediates interactions between hTrio and LAR. Consistent with this observation, we see no significant interactions between Dlar and several fragments of *Drosophila* Trio in an interaction trap assay (N. Kaufmann, J. B., and D. V. V., unpublished data). However, our previous results show that both Abl and Ena can bind directly to the Dlar cytoplasmic domain (Wills et al., 1999b). This fact, coupled with the dramatic genetic interactions between *trio*, *Abl*, and *ena* (Liebl et al., 2000), suggests an alternative possibility, whereby Trio recruitment to the membrane is mediated by one or more Abl pathway components.

Trio and GTPase Interactions

Previous work has shown that different Rho subfamilies of GTPases have distinct roles in the organization of cytoskeletal architecture and cell behavior (reviewed by Hall, 1990). This raises the question of whether Trio coordinates multiple signaling outputs through its two DH domains. In vitro and cellular assays of nucleotide exchange activity using the DH domains of hTrio demonstrated that GEF1 can selectively activate Rac, whereas GEF2 shows specificity for Rho (Debant et al., 1996). In contrast, analysis of the invertebrate Trio-like genes shows that while DH1 GEF function and specificity have been conserved in dTrio and in UNC-73 (Steven et al., 1999; Newsome et al., 2000), the dTrio DH2 domain is not highly active (Newsome et al., 2000). Our analysis of genetic interactions between *trio*, *Drac1*, and *DRho1* in the *Drosophila* retina agrees with these data. Thus, it seems likely that the GEF function of *trio* is mediated primarily by the Rac-like GTPases.

Although no loss-of-function alleles have yet been reported, several Rac-like genes have been identified in *Drosophila*, including *Drac1* and *Drac2* (Luo et al., 1994). Additionally, a third Rac-like gene has been identified in the EST database by the BDGP; this gene shows

closest sequence similarity to the MIG-2 GTPase of *C. elegans* and has been dubbed *mig-two-like* (*mtl*) (Newsome et al., 2000). In *C. elegans*, *mig-2* mutations display overlapping phenotypes and genetic interactions with *unc-73* (Zipkin et al., 1997), consistent with a common function. Both *Drac1* and *mtl* are expressed in the embryonic nervous system of *Drosophila* (Newsome et al., 2000) and are thus candidates for mediating axon guidance functions downstream of *trio*. It is currently unclear whether these GTPases are functionally equivalent or if differential interaction with activators such as *trio* may produce distinct cellular responses. A detailed genetic analysis will be required to distinguish between these possibilities.

Additional Links in Cytoskeletal Signaling

While the functional connection between Trio and Rac-like GTPases provides clear links to cytoskeletal events, recent results suggest that Trio may coordinate the activities of multiple signaling partners. In addition to genetic interactions between *Drosophila trio*, *Abl*, *ena*, and *Dlar* (see above), vertebrate Trio has been shown to bind directly to Filamin (Bellanger et al., 1998b), a protein required for cell motility in a variety of cell types (Cox et al., 1992, 1996; Fox et al., 1998). In addition to forming direct orthogonal cross-links between microfilaments, characteristic of lamellipodia (Hartwig et al., 1975), Filamin also plays a role in RalA GTPase-mediated induction of filopodial structures (Ohta et al., 1999) and interacts with cell surface receptors (e.g., Sharma et al., 1995). Recent data also reveal a role for *Drosophila filamin* in the construction of actin-based structures during oogenesis (Li et al., 1999; Sokol and Cooley, 1999) and in the formation of embryonic axon pathways (N. Sheard, J. B., T. Hays, and D. V. V., unpublished data). Thus, Filamin may provide another direct link between Trio and the cytoskeletal arrays that drive the motile leading edge.

Additional partners for Trio may also come from genetic studies. For example, previous genetic screens (Van Vactor et al., 1993) revealed another gene with a *trio*-like ISNb phenotype called *stop short* (*shot*, also known as *kakapo*; C. Bascom-Slack and D. V. V., unpublished data); recent molecular cloning reveals that this gene encodes a protein with an actin-binding domain (Gregory and Brown, 1998; Strumpf and Volk, 1998). Interestingly, *kakapo* is expressed in the same muscle attachment sites in which we see *trio* expressed (Strumpf and Volk, 1998; see Figure 2), suggesting a functional overlap in different cell types. The shared function of cytoskeletal proteins in many different morphogenetic events is a common theme in many organisms. While these important proteins and signaling pathways are used again and again, their roles in a particular context may be quite specific. Our challenge for the future is to dissect the specific from the general in order to understand the information content of the many pathways that regulate cytoskeletal structure and dynamics.

Experimental Procedures

Drosophila Stocks and Genetics

The P element insertion lines $l(3)S^{1372/3}$ and $l(3)S^{1386/6}$ were obtained from the Szeged outpost of the Umea Stock Centre. *GMR-Drac1* and *GMR-Drho1* lines were a generous gift of the laboratory of Jeffery Settleman. GAL4 expression was controlled by the neuronal-specific *C155-GAL4* (obtained from C. S. Goodman) and the imaginal disc driver *T155-GAL4* (obtained from J. B. Duffy). $UAS\text{-}Drac1^{N17}$ was obtained from L. Luo. All flies were maintained at 25°C.

Immunohistochemistry was carried out as described (Van Vactor and Kopczynski, 1999). Embryos were staged according to Campos-Ortega and Hartenstein (1985). ISNb axons were scored as "stop short" when the trajectory completely failed to contact muscle 12 in the cleft between muscles 12 and 13. This included axons that stalled in the ventral domain before reaching muscle 12 and axons that ignored the target, making ectopic innervations on other local muscles (e.g., muscle 8). The SNa pathway was scored as described in the text. CNS fascicle breaks were scored for all segments in which a distinct fascicle of 1D4-positive axons failed to cross the segment boundary. As with ISNb, abnormally thin fascicles were frequently observed but were scored as wild-type in this analysis.

Isolation of *Drosophila trio*

Single stranded cDNA was synthesized from ~100 μg of total RNA from 12–24 hr embryos using AMV reverse transcriptase (Boehringer Mannheim). Following RNAse treatment, one-fiftieth of the total cDNA reaction was used as a template for degenerate PCR using pfu polymerase (Stratagene), as previously described (Fitzpatrick et al., 1995). The degenerate primer sequences used were 5′-GAR CAYGTNGARGGHGAY-3′ (corresponding to the protein sequence EHVEGD), a forward primer in PH domain 1, and two return primers, 5′-YTTBGGYTTRTTYTGRCARTA-3′ (YCQNKPK) and 5′-YTGYTCR AANAGRAADAT-3′ (IFLFEQ) in GEF2. Total PCR reactions were electrophoresed on agarose gels and blotted to Hybond N^+ membranes (Amersham). For low-stringency Southern hybridization, membranes were incubated for 12 hr in LS buffer (25% formamide, 5× SSC, 5× Denhardt's, 0.1% SDS, and 150 μg/ml salmon sperm DNA) at 40°C, followed by a 24 hr hybridization with radiolabeled hTrio cDNA. Following three washes in 3× SSC at room temperature, blots were subjected to autoradiography at −80°C with an enhancer screen.

Cytological Mapping of *trio*

A nylon filter containing an array of *Drosophila* genomic P1 clones was obtained from Genome Systems and hybridized with a positive fragment obtained from degenerate PCR (corresponding to sequences in DH1). Of four positive clones, three had been previously mapped to the 61E region of chromosome III by in situ hybridization to polytene chromosomes. Furthermore, two sequence-tagged sites (STSs) generated from P1 clones DS04970 and DS02448 correspond to *trio* coding sequence in DH1. The cytological location was confirmed by quantitative Southern analysis using the deficiency *Df(3L)Ar12-1*, which spans 61E.

P Element Mapping

Genomic DNA flanking the P element insertions *P[1372/3]* and *P[1386/6]* was obtained by inverse PCR, as described (Ochman et al., 1988). Insertions were then mapped within 4.5 kb of the 5′ UTR of the *trio* transcript based on hybridization to SalI-digested P1 clones. To more accurately determine the locations of insertion, a PCR product was generated from each P element line using a forward primer extending out from the inverse terminal repeat and a return primer in the 5′ UTR of the transcript. PCR products were then cloned using the TA cloning kit (Invitrogen) and sequenced.

EMS Mutagenesis

w; h2 males that had been isogenized on the third chromosome were fed 25 mM EMS in 1% sucrose overnight, then mated to a *TM3/TM6B* balancer stock. F1 males were then mated to $Df(3L)bab^{PG}/TM6B$, a deficiency with break points 61D3–61F8, and lethality was scored in the F2 generation. Of 7410 independent lines generated, 97 lethal mutations were isolated.

P Element Excision

The P element insertion *P[1372/3]* was remobilized over the balancer *TM3* by introducing transposase on the chromosome $CyO^{HOP2.1}$.

Briefly, *l(3)S*$^{1372/3}$*/TM6B* females were mated to *T(2,3)ES/CyO*$^{HOP2.1}$*; TM3* males to generate +*/CyO*$^{HOP2.1}$*;l(3)S*$^{1372/3}$*/TM3* progeny. Single males and females of this genotype were then crossed to a *TM6B* balancer stock, and *w*$^{-}$*/TM6B* progeny that had lost the P element were obtained in the F2 generation.

Acknowledgments

We thank Barry Dickson, Eric Liebl, Chihiro Hama, and their collaborators for an open exchange of information prior to coordinated submission of our manuscripts. We would also like to thank John Flanagan and Frank Gertler for constructive critique of our manuscript. We are grateful to Michel Streuli and Jeffrey Settleman for providing reagents and information that helped isolate *Drosophila trio*. We also thank Steve Barr and members of the Flanagan Laboratory for many productive intellectual interactions. Many of the stocks used in this work were obtained from the *Drosophila* Stock Center at Bloomington, Indiana, and the Berkekely *Drosophila* Genome Project. D. V. V. is supported by a McKnight Scholar Award; the Council for Tobacco Research, USA; and National Institutes of Health grant NS35909. J. B. was a National Science and Engineering Research Council of Canada Predoctoral Fellow. H. S. is supported by National Institutes of Health grant GM08042.

Received November 23, 1999; revised February 28, 2000.

References

Alam, M.R., Johnson, R.C., Darlington, D.N., Hand, T.A., Mains, R.E., and Eipper, B.A. (1997). Kalirin, a cytosolic protein with spectrin-like and GDP/GTP exchange factor-like domains that interacts with peptidylglycine alpha-amidating monooxygenase, an integral membrane peptide-processing enzyme. J. Biol. Chem. *272*, 12667–12675.

Awasaki, T., Saitoh, M., Sone, M., Suzuki, E., Sakai, R., Ito, K., and Hama, C. (2000). The *Drosophila* Trio plays an essential role in patterning of axons by regulating their directional extension. Neuron *25*, this issue, 119–131.

Barrett, K., Leptin, M., and Settleman, J. (1997). The Rho GTPase and a putative RhoGEF mediate a signaling pathway for the cell shape changes in Drosophila gastrulation. Cell *91*, 905–915.

Bate, M. (1993). The mesoderm and its derivatives. In The Development of *Drosophila melanogaster*, M. Bate and A.M. Arias, eds. (Cold Spring Harbor, NY: Cold Spring Harbor Laboratory Press), pp. 1013–1090.

Bellanger, J.M., Lazaro, J.B., Diriong, S., Fernandez, A., Lamb, N., and Debant, A. (1998a). The two guanine nucleotide exchange factor domains of Trio link the Rac1 and the RhoA pathways in vivo. Oncogene *16*, 147–152.

Bellanger, J.M., Zugasti, O., Lazaro, J.B., Diriong, S., Lamb, N., Sardet, C., and Debant, A. (1998b). Role of the multifunctional Trio protein in the control of the Rac1 and RhoA gtpase signaling pathways. CR Seances Soc. Biol. Fil. *192*, 367–374.

Bentley, D., and Toroian-Raymond, A. (1986). Disoriented pathfinding of pioneer neurone growth cones deprived of filopodia by cytochalasin treatment. Nature *323*, 712–715.

Brand, A.H., and Perrimon, N. (1993). Targeted gene expression as a means of altering cell fates and generating dominant phenotypes. Development *118*, 401–415.

Campos-Ortega, J.A., and Hartenstein, V. (1985). The Embryonic Development of *Drosophila melanogaster* (New York: Springer-Verlag).

Chant, J., and Stowers, L. (1995). GTPase cascades choreographing cellular behavior: movement, morphogenesis, and more. Cell *81*, 1–4.

Chien, C.-B., Rosenthal, D.E., Harris, W.A., and Holt, C.E. (1993). Navigational errors made by growth cones without filopodia in the embryonic Xenopus brain. Neuron *11*, 237–251.

Cox, D., Condeelis, J., Wessels, D., Soll, D., Kern, H., and Knecht, D.A. (1992). Targeted disruption of the ABP-120 gene leads to cells with altered motility. J. Cell Biol. *116*, 943–955.

Cox, D., Wessels, D., Soll, D.R., Hartwig, J., and Condeelis, J. (1996). Re-expression of ABP-120 rescues cytoskeletal, motility, and phagocytosis defects of ABP-120-Dictyostelium mutants. Mol. Biol. Cell *5*, 803–823.

Deak, P., Omar, M.M., Saunders, R.D., Pal, M., Komonyi, O., Szidonya, J., Maroy, P., Zhang, Y., Ashburner, M., Benos, P., et al. (1997). P-element insertion alleles of essential genes on the third chromosome of Drosophila melanogaster: correlation of physical and cytogenetic maps in chromosomal region 86E-87F. Genetics *147*, 1697–1722.

Debant, A., Serra-Pages, C., Seipel, K., O'Brien, S., Tang, M., Park, S., and Streuli, M. (1996). The multidomain protein Trio binds the LAR transmembrane tyrosine phosphatase, contains a protein kinase domain, and has separate rac-specific and rho-specific guanine nucleotide exchange factor domains. Proc. Natl. Acad. Sci. USA *93*, 5466–5471.

Desai, C.J., Gindhart, Jr., J.G., Goldstein, L.S.B., and Zinn, K. (1996). Receptor tyrosine phosphatases are required for motor axon guidance in the Drosophila embryo. Cell *84*, 599–609.

Desai, C.J., Krueger, N.X., Saito, H., and Zinn, K. (1997a). Competition and cooperation among receptor tyrosine phosphatases control motoneuron growth cone guidance in Drosophila. Development *124*, 1941–1952.

Eaton, S., Auvinen, P., Luo, L., Jan, Y.N., and Simons, K. (1995). Cdc42 and Rac1 control different actin-dependant processes in the *Drosophila* wing disc epithelium. J. Cell Biol. *131*, 151–164.

Eaton, S., Wepf, R., and Simons, K. (1996). Roles for Rac1 and Cdc42 in planar polarization and hair outgrowth in the wing of Drosophila. J. Cell Biol. *135*, 1277–1289.

Fambrough, D., and Goodman, C.S. (1996). The Drosophila *beaten path* gene encodes a novel secreted protein that regulates defasciculation at motor axon choice points. Cell *87*, 1049–1058.

Fan, J., and Raper, J.A. (1995). Localized collapsing cues can steer growth cones without inducing their full collapse. Neuron *14*, 263–274.

Feig, L.A., and Cooper, G.M. (1988). Inhibition of NIH 3T3 cell proliferation by a mutant ras protein with preferential affinity for GDP. Mol. Cell. Biol. *8*, 3235–3243.

Fischer, K.D., Tedford, K., and Penninger, J.M. (1998). Vav links antigen-receptor signaling to the actin cytoskeleton. Semin. Immunol. *10*, 314–327.

Fitzpatrick, K.A., Gorski, S.M., Ursuliak, Z., and Price, J.V. (1995). Expression of protein tyrosine phosphatase genes during oogenesis in Drosophila malanogaster. Mech. Dev. *53*, 171–183.

Fox, J., Lamperti, E.D., Eksioglu, Y.Z., Hong, S.E., Feng, Y., Graham, D.A., Scheffer, I.E., Dobyns, W.B., Hirsch, B.A., Radtke, R.A., et al. (1998). Mutations in filamin 1 prevent migration of cerebral cortical neurons in human periventricular heterotopia. Neuron *21*, 1–20.

Gallo, G., and Letourneau, P.C. (1999). Axon guidance: a balance of signals sets axons on the right track. Curr. Biol. *9*, R490-R492.

Gertler, F.B., Doctor, J.S., and Hoffman, F.M. (1990). Genetic suppression of mutations in the Drosophila abl proto-oncogene homologue. Science *248*, 857–860.

Gertler, F.B., Comer, A.R., Juang, J.-L., Ahern, S.M., Clark, M.J., Liebl, E.C., and Hoffmann, F.M. (1995). enabled, a dosage-sensitive suppressor of mutations in the Drosophila Abl tyrosine kinase, encodes an Abl substrate with SH3 domain-binding properties. Genes Dev. *9*, 521–533.

Gertler, F.B., Niebuhr, K., Reinhard, M., Wehland, J., and Soriano, P. (1996). Mena, a relative of VASP and Drosophila Enabled, is implicated in the control of microfilament dynamics. Cell *87*, 227–239.

Gregory, S.L., and Brown, N.H. (1998). kakapo, a gene required for adhesion between and within cell layers in Drosophila, encodes a large cytoskeletal linker protein related to plectin and dystrophin. J. Cell Biol. *143*, 1271–1282.

Hall, A. (1990). The cellular functions of small GTP-binding proteins. Science *249*, 635–640.

Harden, N., Loh, H.Y., Chia, W., and Lim, L. (1995). A dominant inhibitory version of the small GTP-binding protein Rac disrupts cytoskeletal structures and inhibits developmental cell shape changes in Drosophila. Development *121*, 903–914.

Hartwig, J.H., and Stossel, T.P. (1975). Isolation and properties of actin, myosin, and a new actin binding protein in rabbit alveolar macrophages. J. Biol. Chem. *250*, 5696–5705.

Jin, Z., and Strittmatter, S.M. (1997). Rac1 mediates collapsin-1-induced growth cone collapse. J. Neurosci. *17*, 6256–6263.

Kaufmann, N., Wills, Z.P., and Van Vactor, D. (1998). Drosophila Rac1 controls motor axon guidance. Development *125*, 453–461.

Krueger, N.X., Van Vactor, D., Wan, H., Goodman, C.S., Gelbart, W., and Saito, H. (1996). The transmembrane tyrosine phosphatase DLAR controls motor axon guidance in Drosophila. Cell *84*, 611–622.

Lanier, L.M., and Gertler, F.B. (2000). From Abl to actin: the role of the Abl tyrosine kinase and its associated proteins in growth cone motility. Curr. Opin. Cell Biol., in press.

Lanier, L.M., Gates, M.A., Witke, W., Menzies, A.S., Wehman, A.M., Macklis, J., Kwiatkowski, D., Soriano, P., and Gertler, F.B. (1999). Requirement for Mena in neurulation and commissure formation. Neuron *22*, 313–325.

Letourneau, P.C., and Marsh, L. (1984). Growth of neurites without filopodial or lamellipodial activity in the presence of cytochalasin B. J. Cell Biol. *99*, 2041–2047.

Li, M.G., Serr, M., Edwards, K., Ludmann, S., Yamamoto, D., Tilney, L.G., Field, C.M., and Hays, T.S. (1999). Filamin is required for ring canal assembly and actin organization during Drosophila oogenesis. J. Cell Biol. *146*, 1061–1074.

Liebl, E.C., Forsthoefel, D.J., Franco, L.S., Sample, S.H., Hess, J.E., Cowger, J.A., Chandler, M.P., Jackson, A.M., and Seeger, M.A. (2000). Dosage-sensitive, reciprocal genetic interactions between the *Abl* tyrosine kinase and the putative GEF *trio* reveal *trio*'s role in axon pathfinding. Neuron *25*, this issue, 107–118.

Lin, D.M., Fetter, R.D., Kopczynski, C., Grenninggloh, G., and Goodman, C.S. (1994). Genetic analysis of Fasciclin II in Drosophila: defasciculation, refasciculation and altered fasciculation. Neuron *13*, 1055–1069.

Liu, X., Wang, H., Eberstadt, M., Schuchel, A., Olejniczak, E.T., Meadows, R.P., Schkeryantz, J.M., Janowick, D.A., Harlan, J.E., Harris, E.A.S., et al. (1998). NMR structure and mutagenesis of the N-terminal Dbl homology domain of the nucleotide exchange factor Trio. Cell *95*, 269–277.

Lu, Y., and Settleman, J. (1999). The role of Rho family GTPAses in development: lessons from Drosophila melanogaster. Mol. Cell Biol. Res. Comm. *1*, 87–94.

Luo, L., Liao, Y.J., Jan, L.Y., and Jan, Y.N. (1994). Distinct morphogenetic functions of similar small GTPases: Drosophila Drac1 is involved in axonal outgrowth and myoblast fusion. Genes Dev. *8*, 1787–1802.

Machesky, L.M., and Hall, A. (1996). Rho: a connection between membrane receptor signaling and the cytoskeleton. Trends Bichem. Sci. *6*, 304–310.

McIntire, S.L., Garriga, G., White, J., Jacobson, D., and Horvitz, H.R. (1992). Genes necessary for directed axonal elongation or fasciculation in C. elegans. Neuron *8*, 307–322.

Murphy, A.M., and Montell, D.J. (1996). Cell type–specific roles for Cdc42, Rac and RhoL in Drosophila oogenesis. J. Cell Biol. *133*, 617–630.

Newsome, T.P., Schmidt, S., Dietzl, G., Keleman, K., Åsling, B., Debant, A., and Dickson, B.J. (2000). Trio combines with Dock to regulate Pak activity during photoreceptor axon pathfinding in *Drosophila*. Cell *101*, in press.

Nobes, C.D., and Hall, A. (1995). Rho, Rac, and Cdc42 GTPases regulate the assembly of multimolecular focal complexes associated with actin stress fibers, lamellipodia, and filopodia. Cell *81*, 53–62.

Nolan, K.M., Barrett, K., Lu, Y., Hu, K.Q., Vincent, S., and Settleman, J. (1998). Myoblast city, the Drosophila homolog of DOCK180/CED-5, is required in a Rac signaling pathway utilized for multiple developmental processes. Genes Dev. *12*, 3337–3342.

Ochman, H., Gerber, A.S., and Hartl, D.L. (1988). Genetic applications of an inverse polymerase chain reaction. Genetics *120*, 621–623.

Ohta, Y., Suzuki, N., Nakamura, S., Hartwig, J.H., and Stossel, T.P. (1999). The small GTPase RalA targets filamin to induce filopodia. Proc. Natl. Acad. Sci. USA *96*, 2122–2128.

Pistor, S., Chakraborty, T., Walter, U., and Wehland, J. (1995). The bacterial actin nucleator protein ActA of Listeria monocytogenes contains multiple binding sites for host microfilament proteins. Curr. Biol. *5*, 517–525.

Reinhard, M., Giehl, K., Abel, K., Haffner, C., Jarchau, T., Hoppe, V., Jockush, B.M., and Walter, U. (1995). The proline-rich focal adhesion and microfilament protein VASP is a ligand for profilins. EMBO J. *14*, 1583–1589.

Ridley, A.J., and Hall, A. (1992). The small GTP-binding protein rho regulates the assembly to focal adhesions and actin stress fibers in response to growth factors. Cell *70*, 389–399.

Ridley, A.J., Paterson, H.F., Johnston, C.L., Diekmann, D., and Hall, A. (1992). The small GTP-binding protein rac regulates growth factor–induced membrane ruffling. Cell *70*, 401–410.

Sharma, C.P., Ezzell, R.M., and Arnaout, M.A. (1995). Direct interaction of filamin (ABP-280) with the beta 2-integrin subunit CD18. J. Immunol. *154*, 3461–3470.

Siddiqui, S.S., and Culotti, J.G. (1991). Examination of neurons in wild type and mutants of Caenorhabditis elegans using antibodies to horseradish peroxidase. J. Neurogenet. *7*, 193–211.

Simon, M.A., Bowtell, D.D., Dodson, G.S., Laverty, T.R., and Rubin, G.M. (1991). Ras1 and a putative guanine nucleotide exchange factor perform crucial steps in signaling by the sevenless protein tyrosine kinase. Cell *67*, 701–716.

Sokol, N.S., and Cooley, L. (1999). Drosophila filamin encoded by the cheerio locus is a component of ovarian ring canals. Curr. Biol. *9*, 1221–1230.

Sone, M., Hoshino, M., Suzuki, E., Kuroda, S., Kaibichi, K., Nakagoshi, H., Saigo, K., Nabeshima, Y., and Hama, C. (1997). Still life, a protein in synaptic terminals of Drosophila homologous to GDP–GTP exchangers. Science *275*, 543–547.

Steven, R., Kubiseski, T.J., Zheng, H., Kulkarni, S., Mancillas, J., Ruiz Morales, A., Hogue, C.W., Pawson, T., and Culotti, J. (1998). UNC-73 activates the Rac GTPase and is required for cell and growth cone migrations in C. elegans. Cell *92*, 785–795.

Strumpf, D., and Volk, T. (1998). Kakapo, a novel cytoskeletal-associated protein is essential for the restricted localization of the neuregulin-like factor, vein, at the muscle–tendon junction site. J. Cell Biol. *143*, 1259–1270.

Suter, D.M., and Forscher, P. (1998). An emerging link between cytoskeletal dynamics and cell adhesion molecules in growth cone guidance. Curr. Opin. Neurobiol. *8*, 106–116.

Tear, G. (1999). Neuronal guidance: a genetic perspective. Trends Genet. *15*, 113–118.

Tessier-Lavigne, M., and Goodman, C.S. (1996). The molecular biology of axon guidance. Science *274*, 1123–1133.

Van Vactor, D. (1999). Axon guidance. Curr. Biol. *9*, R797-R799.

Van Vactor, D., and Kopczynski, C. (1999). Techniques for anatomical analysis of the *Drosophila* embryonic nervous system. In A Comparative Methods Approach to the Study of Oocytes and Embryos, J. Richter, ed. (New York: Oxford University Press), pp. 490–513.

Van Vactor, D., and Lorenz, L.J. (1999). The semantics of axon guidance. Curr. Biol. *9*, R201-R204.

Van Vactor, D., Sink, H., Fambrough, D., Tsoo, R., and Goodman, C.S. (1993). Genes that control neuromuscular specificity in Drosophila. Cell *73*, 1137–1153.

Wills, Z., Bateman, J., Korey, C., Comer, A., and Van Vactor, D. (1999a). The tyrosine kinase Abl and its substrate Enabled collaborate with the receptor phosphatase Dlar to control motor axon guidance. Neuron *22*, 301–312.

Wills, Z., Marr, L., Zinn, K., Goodman, C.S., and Van Vactor, D. (1999b). Profilin and the Abl tyrosine kinase are required for motor axon outgrowth in the *Drosophila* embryo. Neuron *22*, 291–299.

Winberg, M.L., Noordermeer, J.N., Tamagnone, L., Comoglio, P.M., Spriggs, M.K., Tessier-Lavigne, M., and Goodman, C.S. (1998). Plexin A is a neuronal semaphorin receptor that controls axon guidance. Cell *95*, 903–916.

Yu, H.H., Araj, H.H., Ralls, S.A., and Kolodkin, A.L. (1998). The transmembrane semaphorin Sema I is required in *Drosophila* for embryonic motor and CNS axon guidance. Neuron *20*, 207–220.

Zipkin, I.D., Kindt, R.M., and Kenyon, C.J. (1997). Role of a new Rho family member in cell migration and axon guidance in C. elegans. Cell *90*, 883–894.